BRIEF REPORT

Effect of Gene Therapy on Visual Function in Leber Congenital Amaurosis

James W.B. Bainbridge, Ph.D., F.R.C.Ophth., Alexander J. Smith, Ph.D., Susie S. Barker, Ph.D., Scott Robbie, M.R.C.Ophth., Robert Henderson, M.R.C.Ophth., Kamaljit Balaggan, M.R.C.Ophth., Ananth Viswanathan, M.D., F.R.C.Ophth., Graham E. Holder, Ph.D., Andrew Stockman, Ph.D., Nick Tyler, Ph.D., Simon Petersen-Jones, Ph.D., Shomi S. Bhattacharya, Ph.D., Adrian J. Thrasher, Ph.D., M.R.C.P., F.R.C.P., Fred W. Fitzke, Ph.D., Barrie J. Carter, Ph.D., Gary S. Rubin, Ph.D., Anthony T. Moore, F.R.C.Ophth., and Robin R. Ali, Ph.D.

SUMMARY

Early-onset, severe retinal dystrophy caused by mutations in *RPE65* is associated with poor vision at birth and complete loss of vision in early adulthood. We administered to three young adult patients subretinal injections of recombinant adeno-associated virus vector 2/2 expressing *RPE65* complementary DNA (cDNA) under the control of a human *RPE65* promoter. There were no serious adverse events. There was no clinically significant improvement in visual acuity or in peripheral visual fields on Goldmann perimetry in any of the three patients. We detected no change in retinal responses on electroretinography. One patient had significant improvement in visual function on microperimetry and on dark-adapted perimetry. This patient also showed improvement in a subjective test of visual mobility. These findings provide support for further clinical studies of this experimental approach in other patients with mutant *RPE65*. (ClinicalTrials.gov number, NCT00643747.)

Leber congenital amaurosis is a term used to describe a group of recessively inherited, severe, infantile-onset rod–cone dystrophies.[1] Mutation of one of several genes, including *RPE65*, causes disease that involves impaired vision from birth[2,3] and typically progresses to blindness in the third decade of life. There is no effective treatment. *RPE65* is expressed in the retinal pigment epithelium and encodes a 65-kD protein that is a key component of the visual cycle,[1,4-8] a biochemical pathway that regenerates the visual pigment after exposure to light.[9-14] A lack of functional RPE65 results in deficiency of 11-*cis* retinal so that rod photoreceptor cells are unable to respond to light. Cone photoreceptor cells may have access to 11-*cis*–retinaldehyde chromophore through an alternative pathway that does not depend on retinal pigment epithelium–derived RPE65,[15,16] thus allowing cone-mediated vision in children with Leber congenital amaurosis. However, progressive degeneration of cone photoreceptor cells ultimately results in loss of cone-mediated vision.

Although the retinal dystrophy caused by defects in *RPE65* is severe, features of the disorder suggest that it may respond to gene-replacement therapy. There is useful visual function in childhood, and retinal imaging suggests that photoreceptor-

From the Institute of Ophthalmology, University College London (J.W.B.B., A.J.S., S.S. Barker, S.R., R.H., K.B., A.V., G.E.H., A.S., S.S. Bhattacharya, F.W.F., G.S.R., A.T.M., R.R.A.); Moorfields Eye Hospital (J.W.B.B., A.V., G.E.H., A.T.M.); the National Institute of Health Research Biomedical Research Centre for Ophthalmology, University College London and Moorfields Eye Hospital (J.W.B.B., G. S.R., A.T.M., R.R.A.); the Department of Civil and Environmental Engineering, University College London (N.T.); and the Institute of Child Health, University College London (A.J.T., R.R.A.) — all in London; Michigan State University, East Lansing, MI (S.P.-J.); and Targeted Genetics Corporation, Seattle (B.J.C.). Address reprint requests to Dr. Ali at Institute of Ophthalmology, University College London, Bath Street, London EC1V 9EL, United Kingdom, or at r.ali@ucl.ac.uk.

Drs. Bainbridge and Smith contributed equally to this article.

This article (10.1056/NEJMoa0802268) was published at www.nejm.org on April 28, 2008.

N Engl J Med 2008;358.

cell death occurs late in the disease process.[3] Gene transfer therefore has the potential to improve visual function as well as preserve existing vision. Gene-replacement therapy has been shown to improve visual function in the Swedish Briard dog, a naturally occurring animal model with mutated *RPE65*.[17] Subretinal delivery of recombinant adeno-associated virus vector containing the *RPE65* cDNA results in improved retinal function and improved vision.[18-22]

The purpose of this study was to determine whether gene therapy for retinal dystrophy caused by *RPE65* mutations was associated with immediately obvious adverse events and whether efficacy could be demonstrated in humans. In this exploratory, open-label, single-center study involving three young adults, each of whom received a single subretinal injection of recombinant adeno-associated virus 2/2.hRPE65p.hRPE65, the primary outcome was safety, and the secondary outcome was evidence of efficacy in terms of visual function.

METHODS

PATIENTS AND STUDY DESIGN

In this study, we included young adults (17 to 23 years of age) with early-onset, severe retinal dystrophy caused by missense mutations in *RPE65* (Table 1 in the Supplementary Appendix, available with the full text of this article at www.nejm.org). We excluded persons with visual acuity in the study eye that was better than 20/120 on the Snellen visual-acuity scale, null mutations, and contraindications to systemic immunosuppression, as well as women who were pregnant or lactating. A National Health Service diagnostic laboratory (Manchester Regional Genetics Laboratory) confirmed the genotypes of potential subjects. In each patient, the eye with the worse acuity was selected as the study eye. The contralateral eye was used as a control.

The study was approved by the U.K. Gene Therapy Advisory Committee, the Medicines and Health Products Regulatory Authority, the Moorfields Research Governance Committee, and the local research ethics committee. All patients gave written informed consent. The study was conducted in compliance with Good Clinical Practice guidelines according to the European Clinical Trials Directive (Directive 2001 EU/20/EC) and the Declaration of Helsinki.

Before administration of the vector, we evaluated the retinal structure and function by means of clinical assessment, retinal imaging, psychophysical techniques, and electrodiagnostic methods. Retinal imaging techniques included color fundus photography, fundus autofluorescence imaging, and optical coherence tomography to determine retinal thickness and integrity. We measured visual acuity, contrast sensitivity, color vision, and cone flicker sensitivities. We investigated the patients' visual fields by means of microperimetry (see the Supplementary Appendix), Goldmann dynamic perimetry, and photopic and scotopic (dark-adapted) automated static perimetry (see the Supplementary Appendix). All testing was performed according to standardized, detailed protocols, with controlled room lighting, a dark-adaptation period, and a fixed sequence of test patterns. Both microperimetry and dark-adapted perimetry are fully automated, so there was little opportunity for experimenter bias. We determined the visual mobility of the patients at different illumination levels by measuring their ability to navigate a simulated street scene (Fig. 1 in the Supplementary Appendix). Electrophysiological evaluation included full-field, pattern, and multifocal electroretinography performed to incorporate the standards and guidelines of the International Society for Clinical Electrophysiology of Vision.

We repeated assessments of visual function and immune status (see below) at 2, 4, 6, and 12 months (the latter for Patient 1 only; Patients 2 and 3 have not yet reached the 12-month point) after administration of the vector. The end point for toxic effects for each patient was a grade 3 adverse event, defined as loss of visual acuity by 15 or more letters according to the Early Treatment Diabetic Retinopathy Study scale (on which 20/20 denotes perfect vision), or severe, unresponsive intraocular inflammation. The end point for efficacy for each patient was defined as any improvement in visual function that was greater than the test–retest difference for each technique. The assay of immune response and detection of disseminated recombinant adeno-associated virus are described in the Supplementary Appendix.

RECOMBINANT ADENO-ASSOCIATED VIRUS AND SUBRETINAL DELIVERY

The tgAAG76 vector is a recombinant adeno-associated virus vector of serotype 2. The vector

contains the human *RPE65* coding sequence driven by a 1400-bp fragment of the human *RPE65* promoter and terminated by the bovine growth hormone polyadenylation site, as described elsewhere.[21] The vector was produced by Targeted Genetics Corporation according to Good Manufacturing Practice guidelines with the use of a B50 packaging cell line,[23] an adenovirus–adeno-associated virus hybrid shuttle vector containing the tgAAG76 vector genome, and an adenovirus 5 helper virus. The vector was filled in a buffered saline solution at a titer of 1×10^{11} vector particles per milliliter and frozen in 1-ml aliquots at –70°C.

Patients 1, 2, and 3 underwent surgery on February 7, April 25, and July 11, 2007, respectively. After three-port vitrectomy, we administered up to 1 ml of recombinant adeno-associated virus vector by means of a subretinal cannula (de Juan, Synergetics) to the subretinal space of one eye, involving up to one third of the total retinal area, including the macula. To reduce the possibility of clinically significant intraocular inflammation, patients were given a 5-week course of oral prednisolone, at a dose of 0.5 mg per kilogram of body weight for 1 week before administration of the vector, 1 mg per kilogram for the first week after administration, 0.5 mg per kilogram for the second week, 0.25 mg per kilogram for the third week, and 0.125 mg per kilogram for the fourth week. Patients received betamethasone and cefuroxime subconjunctivally at the completion of surgery and topical treatment with 0.5% chloramphenicol four times a day for 7 days, 0.1% dexamethasone four times a day for 4 weeks, and 1% atropine twice a day for 7 days after surgery. We performed a clinical examination, fundus photography, and ocular coherence tomography (Stratus OCT, Carl Zeiss Meditec) at frequent intervals in the early postoperative period to monitor for retinal reattachment and to identify any intraocular inflammation.

RESULTS

Each patient had little or no vision in low light from an early age but retained some limited visual function in good lighting conditions. We selected these patients because they retained a limited degree of residual retinal function despite advanced retinal degeneration, and they might therefore be expected to benefit from intervention.

We performed vitrectomy and subretinal injection of the vector without complication in each patient (Fig. 1 and Video 1). The vitreous gel was relatively degenerate; a posterior vitreous detachment was present in Patient 2 and was readily induced in Patients 1 and 3 by active aspiration at the optic disk with the use of the vitreous cutter. To deliver the vector to the relatively well-preserved retina at the posterior pole, we performed a retinotomy superior to the proximal part of the superotemporal vascular arcade. To minimize injection of the vector into the vitreous or choroid, we first induced a small detachment of the neurosensory retina, using Hartmann's solution before injecting up to 1 ml of recombinant adeno-associated virus vector (thus creating a "bleb") through the same single retinotomy. In Patient 2, the bleb of the vector extended spontaneously across the macula. We actively manipulated the bleb in Patients 1 and 3 — to involve the macula — by injecting air into the vitreous cavity. We caused no iatrogenic retinal tears, and we left the vector in situ under fluid without retinopexy or intraocular tamponade. On clinical examination 24 hours after surgery, the induced retinal detachment had almost fully resolved in each patient (Fig. 1A). Optical coherence tomography showed minimal persistent subretinal fluid at the macula that resolved 2 to 3 days after surgery (Fig. 1B). On clinical examination, the appearance of the retinas was unchanged for the duration of the follow-up period (up to 12 months).

We detected no dissemination of the vector, as assessed by means of polymerase-chain-reaction amplification of DNA isolated from samples of tears, serum, and saliva collected 1 day and 30 days after administration of the vector and from semen collected at 30 days (data not shown). We observed mild, self-limiting postoperative intraocular inflammation, which typically follows vitrectomy. There were no other adverse events. We found no evidence of cystoid macular edema clinically or on optical coherence tomography. We detected no specific cellular or humoral immune responses to adeno-associated virus capsid (Fig. 2 in the Supplementary Appendix) or specific humoral responses to the transgene product (Fig. 2 and Table 2 of the Supplementary Appendix). We detected a small increase in nonspecific activation of T cells in two patients, which is consistent with a rebound in the num-

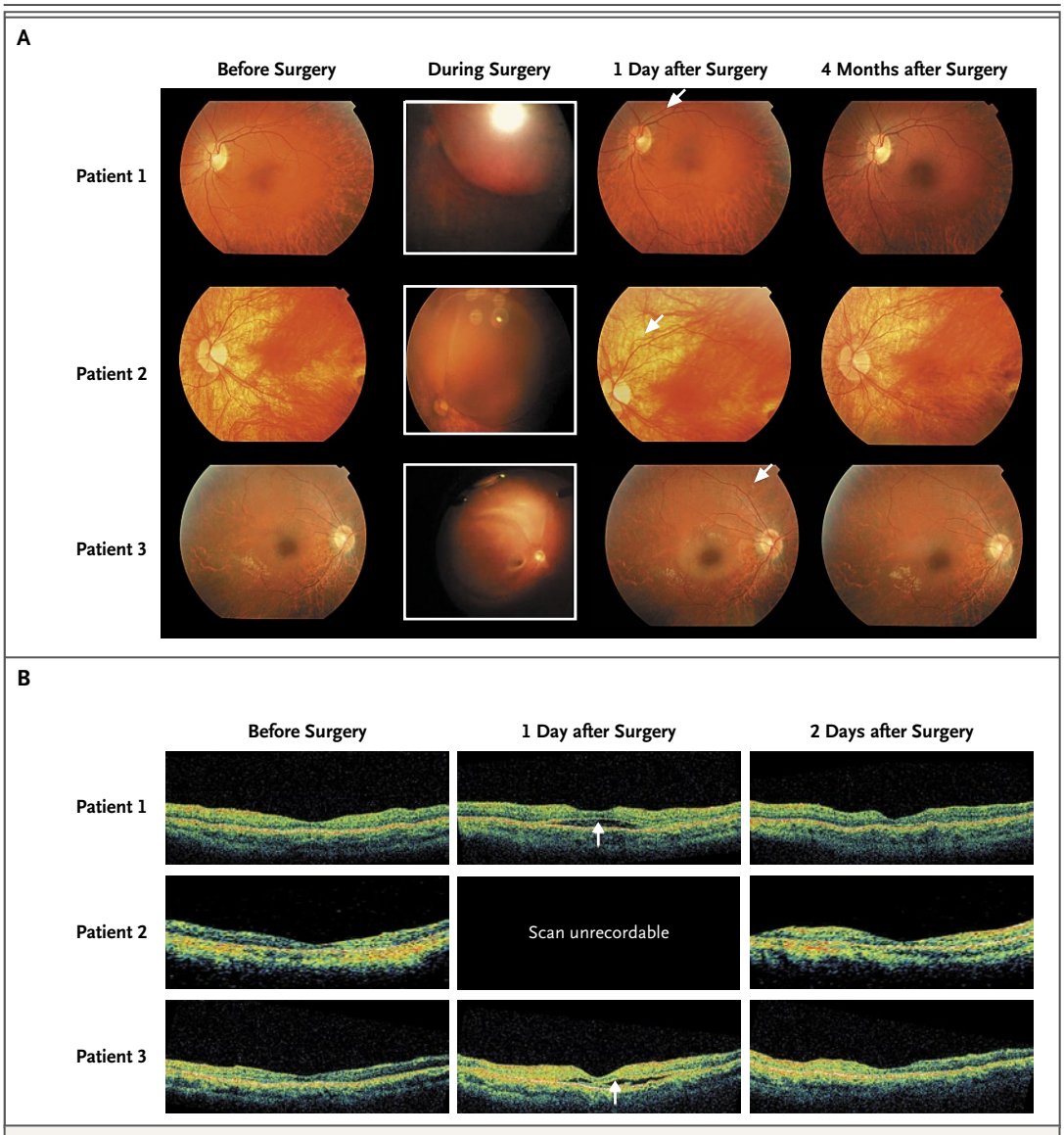

Figure 1. Images of the Fundus and Maculae before and after Experimental Treatment.

In Panel A, fundus photographs show the appearance of the retina in each patient before administration of the vector (before surgery), immediately after subretinal injection of the vector (during surgery), and at 1 day and 4 months after surgery. The site of injection of the vector is indicated by white arrows (see Video 1). Panel B shows cross-sectional images of the retina obtained by optical coherence tomography with the use of six 6-mm radial-line scans and a standardized mapping protocol to show the structure of the retinal layers in each patient. The presence of residual subretinal vector 1 day after surgery is shown (arrows) in Patients 1 and 3 by an area of low signal (black). Images in Patient 2 1 day after surgery were unrecordable because of high-amplitude nystagmus.

bers of some lymphocyte subgroups after the withdrawal of corticosteroids (Fig. 2a in the Supplementary Appendix).

Visual acuity decreased predictably in association with the temporary retinal detachment induced by administration of the vector and returned to preoperative levels by 6 months (Table 1). We observed no clinically significant improvement in visual acuity in any of the three patients (Table 1) or any change in peripheral visual fields on Goldmann perimetry testing. We detected no change in retinal responses to flash or

Table 1. Visual Acuities and Contrast Sensitivities at Baseline and in the Postoperative Period.

Patient No. and Test	Baseline	2 Mo	4 Mo	6 Mo	12 Mo
1					
Study eye — logMAR (Snellen)	1.16 (20/286)	1.06 (20/226)	0.98 (20/190)		0.86 (20/145)
Control eye — logMAR (Snellen)	0.88 (20/150)	0.90 (20/156)	0.68 (20/95)		0.78 (20/120)
Study eye — logCS	0.05	0.30	0.60		0.50
Control eye — logCS	0.55	0.60	0.55		0.55
2					
Study eye — logMAR (Snellen)	1.52 (20/662)	1.50 (20/632)	1.58 (20/760)		1.52 (20/662)
Control eye — logMAR (Snellen)	1.62 (20/833)	1.56 (20/662)	1.52 (20/662)		1.58 (20/760)
Study eye — logCS	0.00	0.00	0.00		0.00
Control eye — logCS	0.00	0.00	0.00		0.00
3					
Study eye — logMAR (Snellen)	0.76 (20/115)	0.90 (20/156)	0.80 (20/126)	0.76 (20/115)	
Control eye — logMAR (Snellen)	0.54 (20/69)	0.46 (20/58)	0.40 (20/50)	0.44 (20/55)	
Study eye — logCS	0.85	0.35	0.45	0.60	
Control eye — logCS	1.10	1.10	1.20	1.10	

* The logarithm of the minimum angle of resolution (logMAR) is used here because it allows comparisons of visual-acuity scores that are more precise than are scores on the Snellen visual acuity scale. LogCS denotes the logarithm of contrast sensitivity.

pattern electroretinography. Before surgery, Patient 2 had high-amplitude nystagmus, which did not change after treatment.

Microperimetry showed no change in retinal function in Patients 1 and 2 but improved retinal function in Patient 3 (Fig. 2A). The baseline data for Patient 3 were obtained from the average of two measurements taken 1 week apart. Measurements were performed on the same retinal loci by registering the fundus image with the baseline image. In an area extending from the outer macula to a point beyond the major vascular arcade, the retinal sensitivity improved progressively in the right (study) eye by as much as 14 dB (a factor of 25). Thus, the patient could see small spots of light that were 1/25th as bright as those that could be seen before treatment. There was no improvement in the left (control) eye.

Dark-adapted perimetry showed no change in retinal function in Patients 1 and 2 but showed improved retinal function in Patient 3 (Fig. 2). In Patients 1 and 2, there was no single location that showed significant improvement or deterioration ($P<0.05$). In Patient 3, some locations in the left (control) eye had yellow bars representing nonsignificant decreases and red bars representing significant decreases in sensitivity. In the right (study) eye, 37 locations showed significant improvements in sensitivity ($P<0.01$). The mean sensitivity at nine locations in the inferonasal region improved from 4 dB at baseline to 26 dB after treatment, and nine locations in the inferotemporal quadrant improved from 7 dB to 28 dB. This finding is equivalent to an improvement in sensitivity of more than 20 dB for these 18 locations, or 100 times the sensitivity threshold observed at baseline.

Visual mobility in low light was unchanged in Patients 1 and 2 but improved in Patient 3 (Fig. 3 and Video 2). In bright conditions, the visually guided mobility in Patient 3 was within normal limits at baseline and follow-up. Under low illumination at baseline, the visual performance of Patient 3 was very poor with the study eye as compared with the control eye (with which he made no errors). At follow-up, we observed a small change for the control eye. We attribute this change to a general learning effect; a similar improvement in travel time to complete the course under dim illumination was also observed in Patient 1. However, after administration of the vector, the travel time for Patient 3 improved

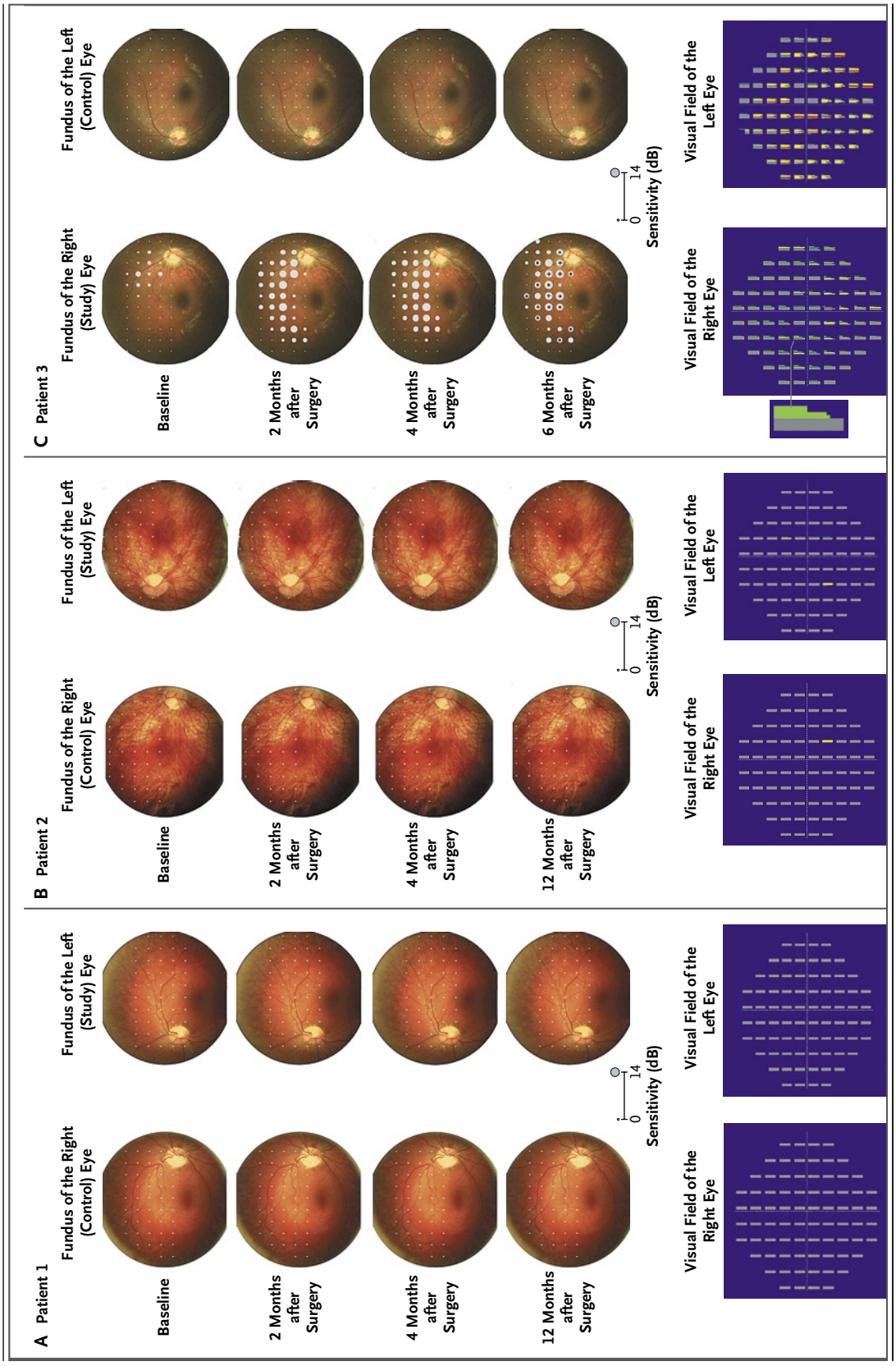
A Patient 1
Fundus of the Right (Control) Eye
Fundus of the Left (Study) Eye
Baseline
2 Months after Surgery
4 Months after Surgery
12 Months after Surgery
Visual Field of the Right Eye
Visual Field of the Left Eye
0
14
Sensitivity (dB)
B Patient 2
Fundus of the Right (Control) Eye
Fundus of the Left (Study) Eye
Baseline
2 Months after Surgery
4 Months after Surgery
12 Months after Surgery
Visual Field of the Right Eye
Visual Field of the Left Eye
0
14
Sensitivity (dB)
C Patient 3
Fundus of the Right (Study) Eye
Fundus of the Left (Control) Eye
Baseline
2 Months after Surgery
4 Months after Surgery
6 Months after Surgery
Visual Field of the Right Eye
Visual Field of the Left Eye
0
14
Sensitivity (dB)

Figure 2 (facing page). Assessment of Visual Function by Microperimetry and Dark-Adapted Perimetry.

The upper portion of each panel shows the microperimetry results for each patient. The size of the circular symbols indicates retinal sensitivity on a scale of 0 to 14 dB. The change in sensitivity in Patient 3 at each tested location from baseline to 6 months' follow-up was evaluated with pointwise linear regression. Of the 55 locations that were tested, 12 (indicated by asterisks) had significant positive slopes ($P<0.05$), ranging from 12 to 28 dB per year. We would expect no more than three points to pass this test by chance alone. A major change in sensitivity of 9 dB or more (an increase in sensitivity by a factor of 8) is indicated by a plus sign. The lower portion of each panel shows the dark-adapted perimetry results for each patient. The analysis provides significance levels for change over time at each individual test location. We made a series of eight measurements during the 6-month follow-up period. Each measurement is depicted by a bar; the lengths of the bars represent sensitivity, with the long bars showing loss of sensitivity and the short bars showing normal sensitivity. Yellow indicates a decline in sensitivity that is not significant, red indicates a decline that is significant ($P<0.05$), and green indicates an improvement that is significant ($P<0.01$). One example, at the X/Y coordinate (–9, +3) of the right eye of Patient 3, is magnified to show the sensitivity measurements going from baseline on the left sequentially through the follow-up assessments on the right. In this example, the long gray bars on the left indicate that the patient was unable to see the light stimulus at maximum intensity. The shorter bars on the right indicate progressive improvement in sensitivity ($P<0.01$).

from 77 seconds to 14 seconds for the study eye, and mobility errors decreased from 8 to 0. Similar results were obtained in a second follow-up test 4 weeks later.

DISCUSSION

Recombinant adeno-associated virus 2/2 vector efficiently transduces retinal pigment epithelial cells after subretinal delivery in animal models.[24] We investigated the feasibility of subretinal vector injection in patients with advanced retinal degeneration and found that we could achieve this outcome predictably and without immediate adverse events, using a transvitreal, transretinal approach after pars plana vitrectomy. A relatively degenerate vitreous facilitated detachment and removal of the posterior vitreous cortex, which otherwise might have resisted passage of the fine cannula. We found that we could deliver through a single retinotomy up to 1 ml of vector subretinally without causing tears in thinned, degenerate retina. To investigate the effect of *RPE65* gene therapy on macular function, we included the macula in the area of vector administration by injection of air into the vitreous cavity when necessary. An important concern was that detachment of the neurosensory retina as a result of subretinal injection could adversely affect vision in the long term, particularly if the detachment involved the macula. We found that the induced retinal detachment resolved spontaneously and fully within a few days after injection, with subsequent recovery of vision to preexisting levels. We did not identify any clinically significant adverse effect of subretinal vector delivery, and the absence of systemic dissemination suggests that any extraocular leakage of vector from the subretinal space was minimal.

To minimize the possibility of intraocular inflammation elicited by vector capsid proteins, we used perioperative systemic immunosuppressive agents. Because of concerns about the possibility of immune responses to the transgene product, we used a tissue-specific promoter and excluded patients with null mutations. We observed no clinically significant intraocular inflammation and detected no immune responses to either adeno-associated virus capsid or RPE65.

We found consistent evidence, on the basis of both microperimetry and dark-adapted perimetry, of improved vision in one patient (Patient 3). The improvement in his visual mobility in low light was also substantially greater than that which would be due to a modest learning effect and was consistent with the improvement in visual function established by means of perimetry. It is not clear whether the improvement in visual responses in the peripheral macula is rod-mediated or cone-mediated. Neither can we be sure that the improvement in visual function is entirely due to enhanced levels of RPE65 in the retina. Evidence for this could be obtained only by biopsy of retinal material, which would be unsafe and unethical. Central macula function and visual acuity did not improve, despite exposure of this region to the vector; this may be due either to amblyopia (i.e., the study eye was amblyopic) or to a requirement for higher levels of RPE65 at the fovea. Visual function improved in only one patient (Patient 3); he had better baseline visual acuity in both the study (amblyopic) eye and the control eye than either of the other patients. He

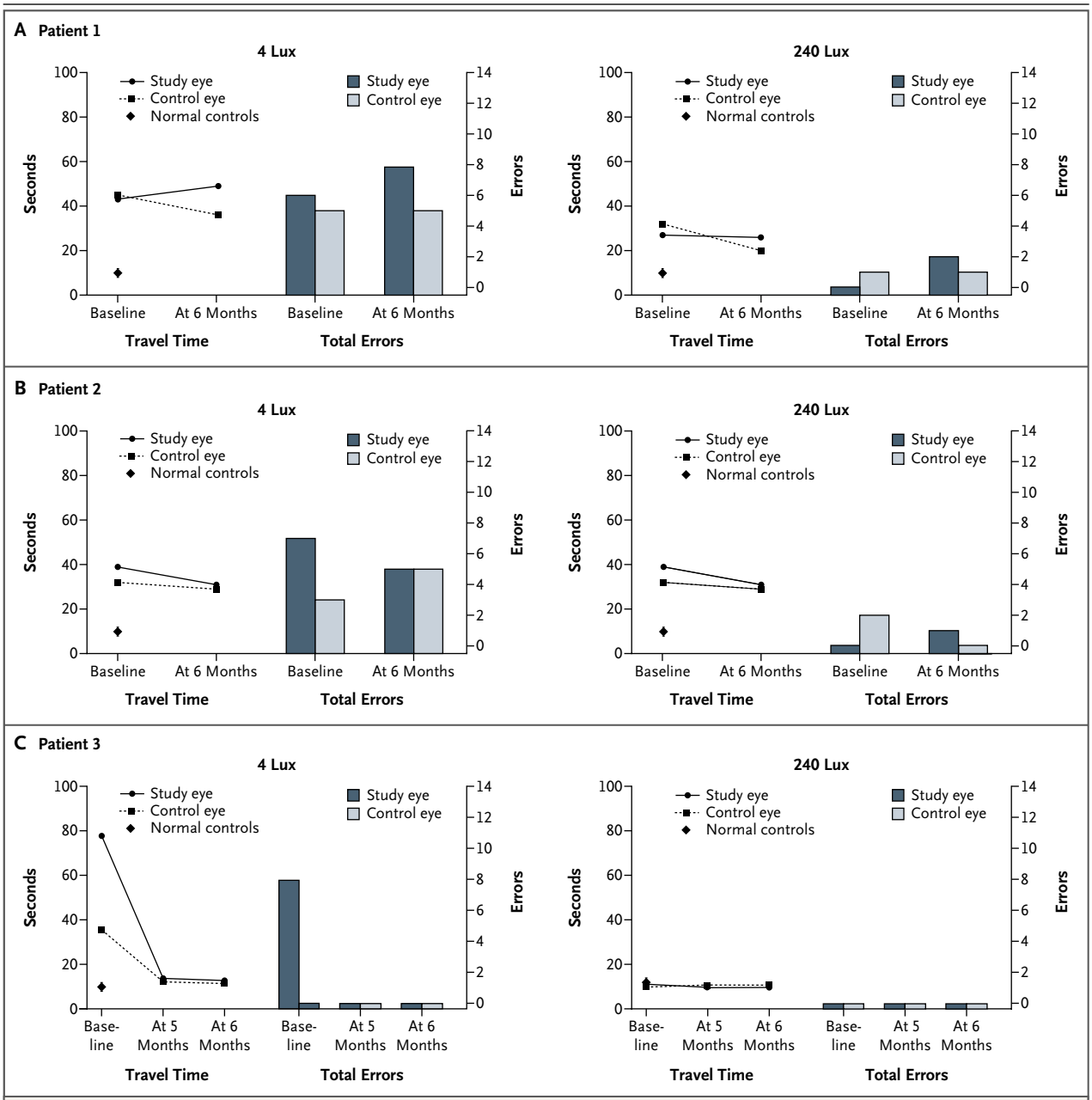

Figure 3. Assessment of Visual Mobility.

Visually guided mobility was assessed at the Pedestrian Accessibility and Movement Environment Laboratory at University College London (see Fig. 1 in the Supplementary Appendix). Panels A, B, and C show data for Patients 1, 2, and 3, respectively, at ambient illumination levels of 4 lux and 240 lux. Average travel times for completing the course (±1 SD) for five control subjects are indicated.

was not the youngest patient, but he probably had less advanced retinal disease at baseline, which may explain why the improvement in this patient was not observed in the other patients. Whether further retinal degeneration is delayed in any of the patients will become apparent only after several years.

The results of this study suggest that subretinal administration of recombinant adeno-associated virus vector is not associated with imme-

diate adverse events in patients with severe retinal dystrophy and that adeno-associated virus–mediated *RPE65* gene therapy can lead to modest improvements in visual function, even in patients with advanced degeneration. Our findings provide support for the development of further clinical studies in children with RPE65 deficiency; these children are more likely to benefit than adults.

Supported by grants from the U.K. Department of Health, the British Retinitis Pigmentosa Society, and the Special Trustees of Moorfields Eye Hospital, and by the Sir Jules Thorn Charitable Trust, the Wellcome Trust, the European Union (EVI-Genoret and Clinigene programs), the Medical Research Council, Foundation Fighting Blindness, Fight for Sight, the Ulverscroft Foundation, Fighting Blindness (Ireland), Moorfields Eye Hospital, and Institute of Ophthalmology Biomedical Research Centre for Ophthalmology, University College London.

Dr. Bainbridge reports being a Wellcome Advanced Fellow and Dr. Thrasher reports being a Wellcome Senior Fellow; Drs. Bainbridge and Ali report being the inventors associated with a U.S. patent application assigned to University College London and Targeted Genomics Corporation entitled, "Devices and methods for delivering polynucleotides into retinal cells of the macula and fovea"; Drs. Fitzke and Viswanathan report being two of the inventors of Progressor software, the intellectual property rights for which are owned by University College London and Moorfields Eye Hospital and licensed to Medisoft; Dr. Carter reports being an employee of Targeted Genetics Corporation. No other potential conflict of interest relevant to this article was reported.

We thank Andrew Dick and the U.K. RPE65 Gene Therapy Data and Safety Monitoring Committee; Alan Bird and the Moorfields Eye Hospital RPE65 Gene Therapy Advisory Committee; Vivien Perry and Moorfields Pharmaceuticals; Graeme Black, for help with genotyping; David Wong, for advice on surgical techniques; and the patients and their families for their effort and commitment.

APPENDIX

The following investigators, who are members of the Moorfields Eye Hospital and University College London Eye Gene Therapy Study Group, participated in this trial: G.W. Aylward, D. Boampong, C. Broderick, P. Buch, C. Childs, Y. Duran, D. Ehlich, S. Falk, M. Feely, T. Fujiyama, F. Ikeji, V. Luong, A. Milliken, R. Maclaren, P. Moradi, F. Mowat, M. Richardson, C. Ripamonti, A. G. Robson, H. Rostron, I. Russell-Eggitt, P. Schlottmann, M. Tschernutter, and N. Wasseem.

REFERENCES

1. Hanein S, Perrault I, Gerber S, et al. Leber congenital amaurosis: comprehensive survey of the genetic heterogeneity, refinement of the clinical definition, and genotype-phenotype correlations as a strategy for molecular diagnosis. Hum Mutat 2004;23:306-17.

2. Lorenz B, Gyürüs P, Preising M, et al. Early-onset severe rod-cone dystrophy in young children with RPE65 mutations. Invest Ophthalmol Vis Sci 2000;41:2735-42.

3. Paunescu K, Wabbels B, Preising MN, Lorenz B. Longitudinal and cross-sectional study of patients with early-onset severe retinal dystrophy associated with RPE65 mutations. Graefes Arch Clin Exp Ophthalmol 2005;243:417-26.

4. Thompson DA, Gyürüs P, Fleischer LL, et al. Genetics and phenotypes of RPE65 mutations in inherited retinal degeneration. Invest Ophthalmol Vis Sci 2000;41:4293-9.

5. Gu SM, Thompson DA, Srikumari CR, et al. Mutations in RPE65 cause autosomal recessive childhood-onset severe retinal dystrophy. Nat Genet 1997;17:194-7.

6. Marlhens F, Bareil C, Griffoin JM, et al. Mutations in RPE65 cause Leber's congenital amaurosis. Nat Genet 1997;17:139-41.

7. Morimura H, Fishman GA, Grover SA, Fulton AB, Berson EL, Dryja TP. Mutations in the RPE65 gene in patients with autosomal recessive retinitis pigmentosa or Leber congenital amaurosis. Proc Natl Acad Sci U S A 1998;95:3088-93.

8. Lotery AJ, Namperumalsamy P, Jacobson SG, et al. Mutation analysis of 3 genes in patients with Leber congenital amaurosis. Arch Ophthalmol 2000;118:538-43.

9. Thompson DA, Gal A. Genetic defects in vitamin A metabolism of the retinal pigment epithelium. Dev Ophthalmol 2003;37:141-54.

10. Redmond TM, Yu S, Lee E, et al. Rpe65 is necessary for production of 11-cis-vitamin A in the retinal visual cycle. Nat Genet 1998;20:344-51.

11. Mata NL, Moghrabi WN, Lee JS, et al. Rpe65 is a retinyl ester binding protein that presents insoluble substrate to the isomerase in retinal pigment epithelial cells. J Biol Chem 2004;279:635-43.

12. Jin M, Li S, Moghrabi WN, Sun H, Travis GH. Rpe65 is the retinoid isomerase in bovine retinal pigment epithelium. Cell 2005;122:449-59.

13. Moiseyev G, Chen Y, Takahashi Y, Wu BX, Ma JX. RPE65 is the isomerohydrolase in the retinoid visual cycle. Proc Natl Acad Sci U S A 2005;102:12413-8.

14. Redmond TM, Poliakov E, Yu S, Tsai JY, Lu Z, Gentleman S. Mutation of key residues of RPE65 abolishes its enzymatic role as isomerohydrolase in the visual cycle. Proc Natl Acad Sci U S A 2005;102:13658-63.

15. Znoiko SL, Crouch RK, Moiseyev G, Ma JX. Identification of the RPE65 protein in mammalian cone photoreceptors. Invest Ophthalmol Vis Sci 2002;43:1604-9.

16. Wu BX, Moiseyev G, Chen Y, Rohrer B, Crouch RK, Ma JX. Identification of RDH10, an all-trans retinol dehydrogenase, in retinal Muller cells. Invest Ophthalmol Vis Sci 2004;45:3857-62.

17. Veske A, Nilsson SE, Narfström K, Gal A. Retinal dystrophy of Swedish Briard/Briard-beagle dogs is due to a 4-bp deletion in RPE65. Genomics 1999;57:57-61.

18. Acland GM, Aguirre GD, Ray J, et al. Gene therapy restores vision in a canine model of childhood blindness. Nat Genet 2001;28:92-5.

19. Narfström K, Katz ML, Bragadottir R, et al. Functional and structural recovery of the retina after gene therapy in the RPE65 null mutation dog. Invest Ophthalmol Vis Sci 2003;44:1663-72.

20. Narfström K, Katz ML, Ford M, Redmond TM, Rakoczy E, Bragadottir R. In vivo gene therapy in young and adult RPE65–/– dogs produces long-term visual improvement. J Hered 2003;94:31-7.

21. Le Meur G, Stieger K, Smith AJ, et al. Restoration of vision in RPE65-deficient Briard dogs using an AAV serotype 4 vector that specifically targets the retinal pigmented epithelium. Gene Ther 2007;14:292-303.

22. Aguirre GK, Komáromy AM, Cideciyan AV, et al. Canine and human visual cortex intact and responsive despite early retinal blindness from RPE65 mutation. PLoS Med 2007;4(6):e230.

23. Gao GP, Qu G, Faust LZ, et al. High-titer adeno-associated viral vectors from a Rep/Cap cell line and hybrid shuttle virus. Hum Gene Ther 1998;9:2353-62.

24. Auricchio A, Rolling F. Adeno-associated viral vectors for retinal gene transfer and treatment of retinal diseases. Curr Gene Ther 2005;5:339-48.

Supplementary Appendix

This appendix has been provided by the authors to give readers additional information about their work.

Supplement to: Bainbridge JWB, Smith AJ, Barker SS, et al. Effect of gene therapy on visual function in Leber congenital amaurosis. N Engl J Med 2008;358. DOI: 10.1056/NEJMoa0802268.

SUPPLEMENTARY INFORMATION

Supplementary Methods

Microperimetry

Microperimetry was performed using a Nidek MP1 microperimeter (NAVIS software version 1.7.1, Nidek Technologies, Padova, Italy). Following 10 minutes of dark adaptation a white fixation cross (31.8 cd/m^2) was displayed on a dim background (1.27 cd/m^2). Goldman V stimuli of 200 ms duration and a maximum luminance of 127 cd/m^2 were presented with a 4-2 adaptive staircase thresholding strategy. All testing followed a standardised, detailed protocol, with controlled room lighting, dark-adaptation period and a fixed sequence of test patterns. The test is fully automated so there is little opportunity for experimenter bias. The subject's eye position was continually monitored by an infrared camera and the microperimeter tracks the eye movements to compensate for shifts in the direction of gaze. Reliability parameters were determined for each test including fixation losses, false negative and false positive responses. Test reliability was assessed by projecting a light onto a known blind spot (the optic nerve head); positive responses to the light indicate poor reliability.

Dark-adapted perimetry

In dark-adapted conditions using a short wave length stimulus, sensitivities were measured at 76 locations in the central visual field using a modified Humphrey perimeter. Measurements were made between 60 and 240 minutes dark adaptation using Goldman V stimuli of 200 ms duration. All testing followed a standardised, detailed protocol, with controlled room lighting, dark-adaptation period and a fixed sequence of test patterns. The test is fully automated so there is little opportunity for experimenter bias. The subject's eye position was continually monitored by an infrared camera. Reliability parameters were determined for each test including fixation losses, false negative and false positive responses. Test reliability was assessed by projecting a light onto a known blind spot (the optic nerve head); positive responses to the light indicate poor reliability.

Assessment of visual mobility

(see Supplementary Figure 1)

PAMELA is a unique mobility research facility (in a specially designed, converted warehouse building) that incorporates a sophisticated set of monitoring and data collection systems including starlight video cameras, Laser scanners which can locate objects in the laboratory within 1-2cm, eye tracking systems and heart rate monitors. To ensure consistent light levels the illumination of the platform was measured before and after testing, and found to vary by less than 5% overall and less than 3% in the critical area of the mobility maze. Dark adaptation time was held constant across sessions and the maze was randomly configured for each test. Three of the 8 random configurations are illustrated in **Supplementary Figure 1**. The experimenter, though not masked to the treatment eye, stood behind the subject and did not speak to him except to read instruction from a printed script. Visual mobility was tested with a 10.8m x 7.2m raised platform with concrete paving assessed stones that were configured to simulate an outdoor pavement. Subjects negotiated a 13m long maze with 8 moveable barriers (1.8m x 1.2m) painted in colours matching light or dark blue denim, and the entire platform area was illuminated from overhead to calibrated light levels ranging from 240 lux (moderate office lighting) to 4 lux (UK night time pedestrian lighting standard). The subject was positioned at one end of the maze and instructed to walk through at a normal comfortable pace without touching the barriers. The experimenter followed along just behind to ensure the subject's safety. Total travel was recorded with a stopwatch along with mobility errors (touching a barrier, loss of orientation). The barriers were randomly re-positioned before each run and the subject was given 15 minutes to adapt to changes in illumination levels.

Supplementary Figure 1

Schematic of maze used for assessment of visual mobility

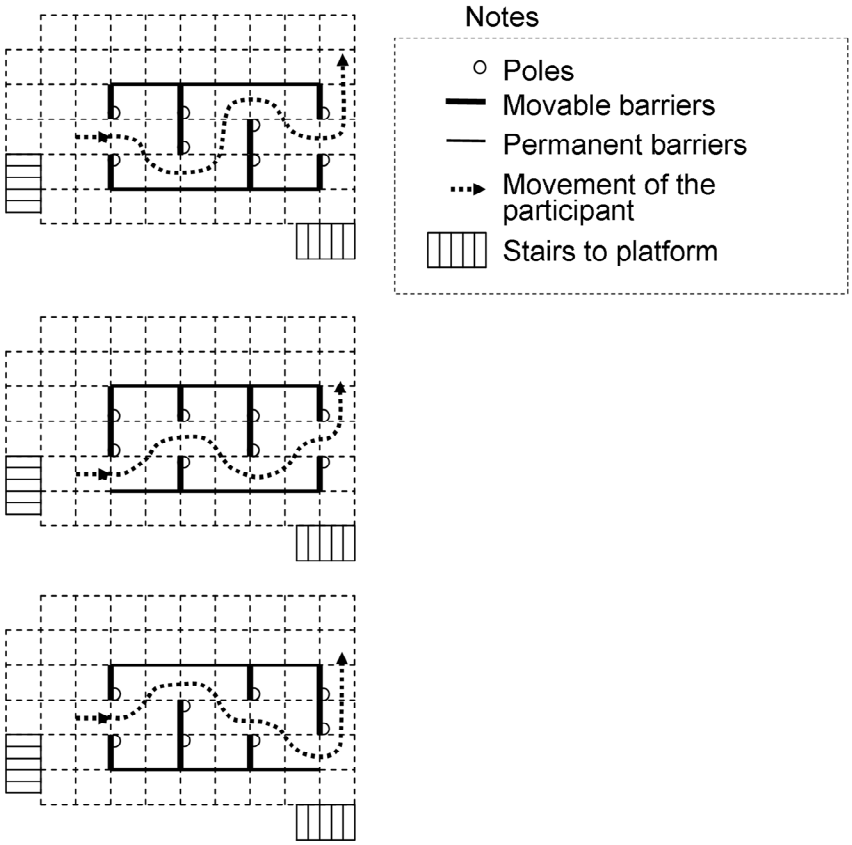

Assay of Immune Response and Detection of Disseminated rAAV

To investigate possible systemic cellular and humoral immune responses to rAAV, we performed baseline ELISpot and ELISA and neutralising antibody assays on samples of the subjects' blood and serum. ELISpot assays were performed to detect adaptive cellular immune responses by measuring IFNγ secretion by PBMC following co-culture with intact vector particles. Humoral responses were investigated by ELISA to detect total circulating IgA, IgG and IgM against AAV2 or rRPE65, and by detection of neutralising antibodies against AAV2, which might inhibit vector transduction. We investigated dissemination of vector by PCR amplification of vector genomes isolated from samples of tears, serum and saliva collected 1 day and 30 days following vector administration, and from semen collected at 30 days.

Supplementary Figure 2a

ELISpot assay to detect cytokine expression in PBMCs in response to co-culture with AAV2

None of the subjects displayed a specific increase in the number of IFNγ secreting cells following co-culture of PBMCs with intact AAV2 particles. PVDF plates were coated with anti-IFNγ and blocked with FCS. PBMC were resuspended in serum-free media and 2.5 x 10^5 cells added per well. Positive controls contained anti-CD3 and negative controls were incubated in media only. Triplicate test wells contained 10^7 intact vector particles. Plates were incubated at 37°C for 48 h. Plates were developed using an avidin-alkaline phosphatase detection system following a biotinylated detection antibody. The data shows the average spots per well of triplicate test wells ± SD. Test wells with more than double the number of spots in the negative controls were considered to be a positive response against antigen. This assay shows that AAV2-specific T-cell responses are not generated by the subjects' PBMCs following co-culture with the AAV2 vector. An increase in non-specific activation was observed in subject 1 and subject 3 at week 8 and 16. This is consistent with a rebound in the numbers of some lymphocyte subsets after removal of steroids. The effects observed at week 52 in subject 1 may be due to a respiratory infection the patient had suffered 2-3 weeks before the blood sample was taken. The increased activation observed in the negative control well indicates the increase in IFNγ expression was not in response to AAV2.

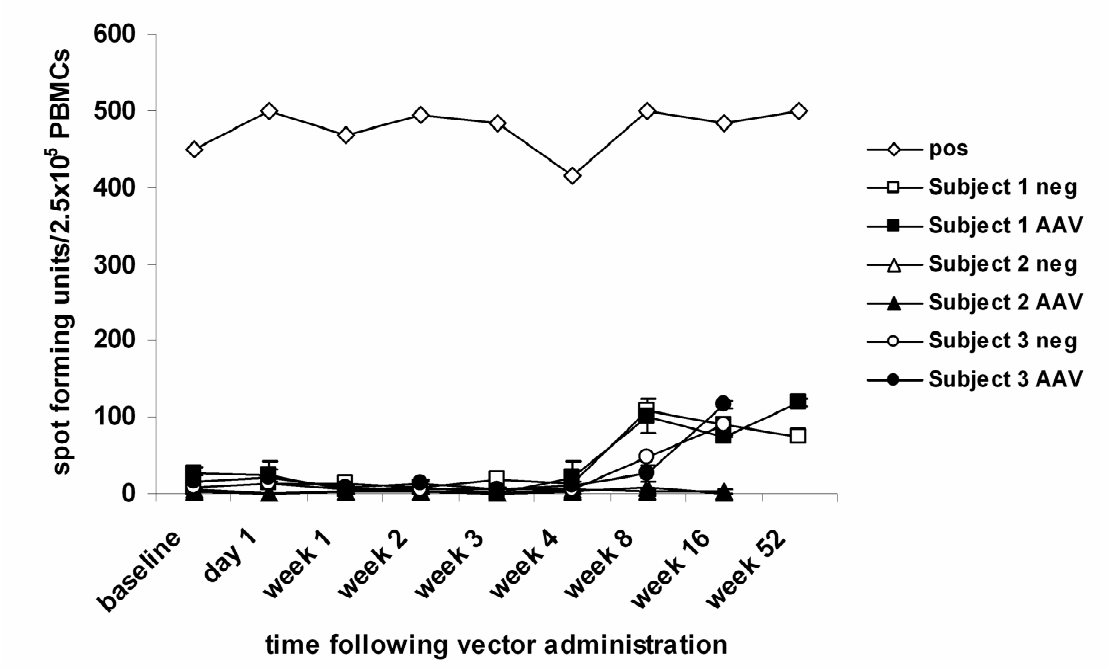

Supplementary Figure 2b

ELISA to detect circulating levels of IgA, IgG and IgM against AAV2 or rRPE65

None of the subjects showed any increase in circulating IgA, IgG or IgM against either vector or transgene. Serum was isolated from the same sample used for PBMC isolation and tested at the same time points for antibodies against AAV2 and recombinant human RPE65. Microtitre plates were coated with 50,000 vp/well AAV2 or 0.5µg/ml rRPE65 then blocked with 50% goat serum in PBS. Serum dilutions were added to wells (replicates of 6) and incubated for 2 h. Plates were incubated with anti-human IgA, IgG, IgM, then developed with TMB substrate. Data is expressed as the relative antibody titre compared with baseline samples obtained before vector administration and run alongside each assay.

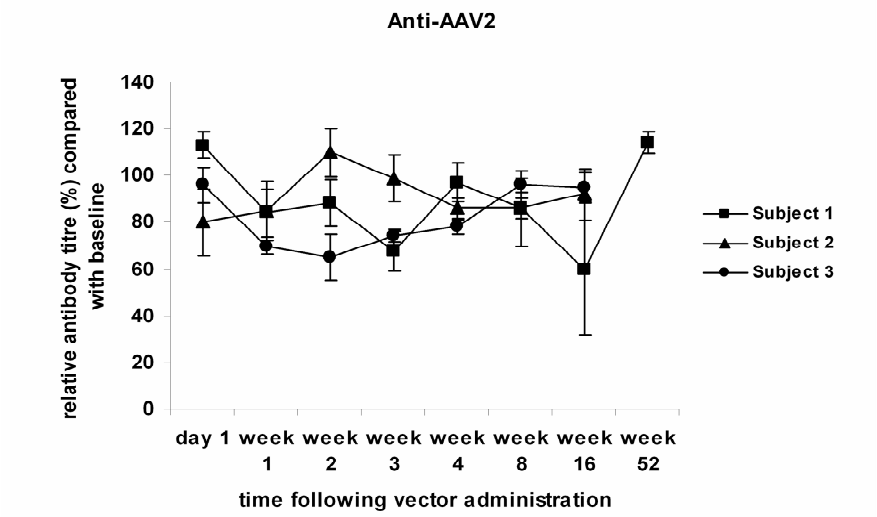

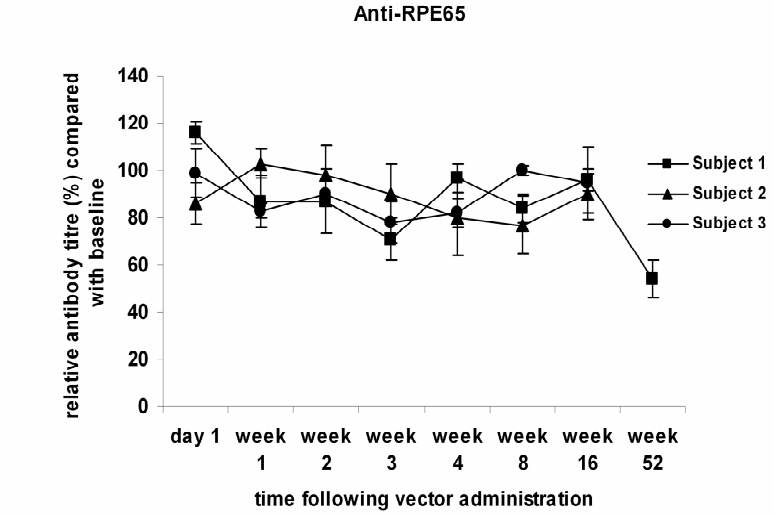

Supplementary Table 1

Subject characteristics at baseline

							ERG		
Sub.	**Age (Yrs)**	**Sex**	**Mutation**	**Amino acid change**	**VA (Log MAR)**	**Refractive error**	**Rods (Bright flash)**	**Cones (30Hz flicker)**	**Macula (PERG/ Multifocal)**
1	23	M	homozygous c. [1102T>C]	p. Tyr368His	1.16	-3.75 / -0.50 x 170	No definite response	Residual	Undetectable
2	17	F	c. [11+5G>A] + [118G>A]	Splice site p. Gly40Ser	1.52	+1.50 / -1.00 x 90	Residual	Very reduced & delayed (4.0µV; 41ms)	Untestable (nystagmus)
3	18	M	c. [16G>T] + [499G>T]	p. [Glu6X] + [Asp167Tyr]	0.76	-0.25 / -2.00 x 52	No definite response	Very reduced & delayed (10µV; 42ms)	Undetectable

Supplementary Table 2

Neutralising AAV-2 antibody titre

None of the subjects show an increase in humoral responses to AAV2. Serum was assayed for the ability to block the transduction of 293T cells with AAV2-GFP. Serum was serially diluted in multi-well plates using DMEM. AAV2-GFP was added to each well and plates were incubated at 37°C for 1 h before addition to 293T cells in triplicate. The NAb titre was expressed as the serum dilution that resulted in 50% inhibition of transduction by AAV2-GFP. Baseline serum from each subject was assayed alongside each post-op sample. Green cells were counted in the test wells after 48 h and compared with the number of green cells in the baseline serum sample. Subject 1 showed a baseline titre of 1:4, and this remained at around the same level 1 year after vector administration. Subjects 2 and 3 had undetectable levels of NAb before vector delivery, and the titre remained undetectable for the duration of follow-up.

	Subject 1		Subject 2		Subject3	
	50% inhibition	0% inhibition	50% inhibition	0% inhibition	50% inhibition	0% inhibition
Baseline pre-op	1:4	1:8	No inhibition detected	Neat serum	No inhibition detected	Neat serum
Day 1	1:3	1:4	No inhibition detected	Neat serum	No inhibition detected	Neat serum
Week 1	1:3	1:4	No inhibition detected	Neat serum	No inhibition detected	Neat serum
Week 2	1:4	1:10	No inhibition detected	Neat serum	No inhibition detected	Neat serum
Week 3	1:4	1:8	No inhibition detected	Neat serum	No inhibition detected	Neat serum
Week 4	1:6	1:16	1:2	Neat serum	No inhibition detected	Neat serum
Week 8	1:5	1:8	No inhibition detected	Neat serum	No inhibition detected	Neat serum
Month 4	1:6	1:10	No inhibition detected	Neat serum	No inhibition detected	Neat serum
Year 1	1:4	1:10	N/A	N/A	N/A	N/A

Supplementary Video 1

Vitrectomy and subretinal injection of rAAV vector

SEE VIDEO

This video demonstrates the surgical technique used to administer vector. We performed a 3-port 20-gauge pars plana vitrectomy and used a 41-gauge de Juan cannula to make a retinotomy superior to the proximal part of the superotemporal vascular arcade. In subjects 1 and 3 we induced a posterior vitreous detachment. In subject 2 a posterior vitreous detachment was already present. To minimise injection of vector into the vitreous or choroid, we first induced a small detachment of the neurosensory retina ('bleb') using Hartmann's solution before injecting up to 1 ml rAAV vector via the same single retinotomy. In subject 2 the bleb of vector extended spontaneously across the macula. In subjects 1 and 3 we actively manipulated the bleb to involve the macula by injecting air into the vitreous cavity. We left the vector *in-situ* under fluid without retinopexy or intraocular tamponade.

Supplementary Video 2

Assessment of visual mobility

SEE VIDEO

Video showing performance of subject 3 during the visual mobility task. The subject was instructed to walk at a normal comfortable pace along a 13 m route whilst avoiding 8 moveable barriers arranged in a simple maze. Testing was monocular with the fellow eye occluded by an opaque eye patch. The subject wore a helmet-mounted eye tracker that followed the direction of gaze. The maze was illuminated from overhead to a calibrated average light level of 4 lux (UK night time pedestrian lighting standard). The first section of the video shows performance with the study eye at baseline. The subject required 77 seconds to traverse the maze and made 8 errors (bumps or losses of orientation). The second section shows performance with the study eye 6 months after treatment. The subject required only 14 seconds to navigate the maze and made no errors. This was comparable to performance by normal controls who take 10 (±2) seconds.